LLaVA-Ultra: Large Chinese Language and Vision Assistant for Ultrasound

Xuechen Guo
ZJU-UIUC Institute, Zhejiang University
Haining, Zhejiang, China
xuechen.22@intl.zju.edu.cn

Wenhao Chai
University of Washington
Seattle, Washington, USA
wchai@uw.edu

Shi-Yan Li*
Zhejiang University School of Medicine Sir Run Run Shaw Hospital
Hangzhou, Zhejiang, China
lishiyan@zju.edu.cn

Gaoang Wang*
ZJU-UIUC Institute, Zhejiang University
Haining, Zhejiang, China
Shanghai Artificial Intelligence Laboratory
Shanghai, China
gaoangwang@intl.zju.edu.cn

Abstract

Multimodal Large Language Model (MLLM) has recently garnered attention as a prominent research focus. By harnessing powerful LLM, it facilitates a transition of conversational generative AI from unimodal text to performing multimodal tasks. This boom begins to significantly impact medical field. However, general visual language model (VLM) lacks sophisticated comprehension for medical visual question answering (Med-VQA). Even models specifically tailored for medical domain tend to produce vague answers with weak visual relevance. In this paper, we propose a fine-grained adaptive VLM architecture for Chinese medical visual conversations through parameter-efficient tuning. Specifically, we devise a fusion module with fine-grained vision encoders to achieve enhancement for subtle medical visual semantics. Then we note data redundancy common to medical scenes is ignored in most prior works. In cases of a single text paired with multiple figures, we utilize weighted scoring with knowledge distillation to adaptively screen valid images mirroring text descriptions. For execution, we leverage a large-scale multimodal Chinese ultrasound dataset obtained from the hospital. We create instruction-following data based on text from professional doctors, which ensures effective tuning. With enhanced model and quality data, our **L**arge Chinese **L**anguage **a**nd **V**ision **A**ssistant for **Ultra**sound (LLaVA-Ultra) shows strong capability and robustness to medical scenarios. On three Med-VQA datasets, LLaVA-Ultra surpasses previous state-of-the-art models on various metrics.

CCS Concepts

• **Computing methodologies** → *Visual content-based indexing and retrieval*; *Matching*; *Image representations*.

---

*Corresponding author.

Keywords

Multimodal large language model, Medical instruction tuning

1 Introduction
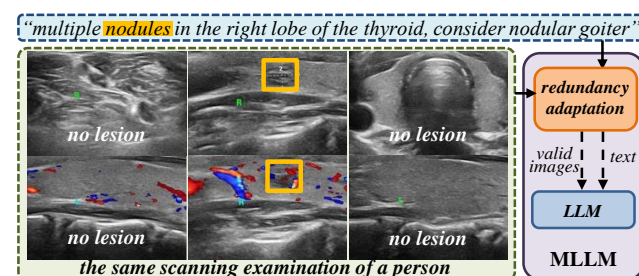
Figure 1: Data redundancy common in medical scenes puts a need for fine-grained perception and adaption in MLLM.

Generative pretraining has demonstrated effective for visual language modeling in the general domain, utilizing image-text multimodal data, as exemplified by GPT-4 [24] and LLaVA [21]. Through self-supervised finetuning with instruction-following data, pretrained Large Language Models (LLMs) [3, 34, 52] can be adapted to unseen tasks, resulting in improved zero-shot performance. This simple yet powerful method has extended to the multimodal field. It gives rise to Multimodal Large Language Models (MLLMs) [1, 11, 45] that excel in visual language tasks such as image reasoning and further forms user-oriented multimodal conversation assistants.

Based on the success of MLLMs in the general domain, similar initiatives have emerged for medical applications [2, 28, 50]. Current research is gradually transitioning from unimodal text to incorporating multimodal medical data. However, despite their effectiveness in general tasks, MLLMs often struggle in medical contexts. This results in inaccuracy or refusal to provide answers when

MM '24, October 28–November 1, 2024, Melbourne, VIC, Australia.

Xuechen Guo, Wenhao Chai, Shi-Yan Li, & Gaoang Wang

faced with medical questions. It is partially due to the scarcity and difficulty in accessing parallel medical image-text data, unlike the diverse internet data available for the general domain. LLaVA-Med [17] alleviates this issue to some extent by creating multimodal medical instruction-following data for finetuning. However, it still struggles to provide more detailed correct responses. Sometimes its answers tend to be vague, focusing more on medical concepts in textual questions rather than in-depth image analysis. From the data perspective, it utilizes image-text data extracted from PubMed public papers, which may be coarser and less cross-modal matched than those from primary sources. Notably, it ignores data redundancy common in clinics shown in Fig. 1 as many other previous works. This puts a need for model enhancement and adaption for the fine-grained medical domain. Additionally, there is little exploration of extensive Chinese data in the medical multimodal field.

In this paper, we propose a **L**arge Chinese **L**anguage **a**nd **V**ision **A**ssistant for **Ultra**sound (LLaVA-Ultra), an end-to-end trained medical multimodal chatbot. To our knowledge, it is the first attempt to extend multimodal finetuning to the Chinese medical domain based on a large-scale dataset. Its domain-specific pretraining has shown effectiveness for medical vision-language (VL) tasks. Specifically, our paper makes the following contributions:

- **Enhancement for medical adaptation**. To meet the needs of subtle medical images, we leverage an extra fine-grained Segment Anything Model (SAM) [16] encoder to jointly extract visual semantics with the CLIP encoder. A followed fusion module can effectively integrate these two typical features and thus achieve visual enhancement for better multimodal alignment. Moreover, for data redundancy common in medical scenarios, we design an adaptive sampling module with weighted scoring and knowledge distillation to automatically screen valid information. It improves the model's robustness and thus ensures correct responses in complicated practical medical scenarios.

- **High-quality medical parallel data.** We present a novel data sourcing pipeline to collect a large-scale Chinese ultrasound multimodal dataset first-hand from the hospital database. It covers professional content provided by doctors for ultrasound examinations of many body parts. We sample pairs of around 1.7M ultrasound images and 188k clinical texts and generate multi-modal instructions with GPT-3.5 [23] for medical instruction-tuning.

- **LLaVA-Ultra**. Contributed by the robust architecture as well as fine-grained professional data, LLaVA-Ultra shows the best practice in the Chinese medical domain. Trained in only 60 hours with 4 48GB A40s, it provides detailed answers relevant to visual content in medical conversations. On our ultrasound hospital dataset and public medical visual question answering (VQA) datasets, LLaVA-Ultra outperforms prior state-of-the-art (SOTA).

2 Related Work

Research of Multimodal Large Language Models (MLLMs) [4, 41, 45] is an emerging hotspot currently. The key concept is to leverage pre-trained Large Language Models (LLMs) to incorporate information from other modalities, such as vision, for performing multimodal tasks like image and video understanding [31, 51] and embodied agent [37, 53–55]. Remarkable works such as BLIP-2 [18], LLaVA [21] and LLAMA-Adpater [48] demonstrate prominent generative abilities including visual question answering (Med-VQA) and image captioning [8, 9]. This has expanded the research of AI into new fields and holds promising prospects for further development [22].

Medical multimodal chatbots. Inspired by these successes, explorations into MLLMs have transitioned into the medical domain, exemplified by models like LLaVA-Med [17] and Med-PaLM M [35]. They utilize medical datasets to perform instruction tuning [27] for MLLMs initialized from the general domain and thus create potential medical applications, such as medical VQA. For instance, LLAVA-Med extends LLaVA to medical domain in this way.

Although LLaVA-Med and our proposed LLaVA-Ultra share a similar base model LLaVA, they differ significantly: (*i*) *Model architecture.* LLaVA-Med is based on the base model LLaVA without significant modifications. However, we propose effective enhancements to the model structure to adapt the characteristics of medical data. It primarily focuses on improving comprehension of subtle visual semantics and adapting to data redundancy in medical scenarios. Thus, our LLaVA-Ultra improves effectiveness and robustness in medical applications. (*ii*) *Data source and characteristic.* LLaVA-Med relies on rougher internet-based data PMC-15M [49], whereas our model utilizes first-hand, specialized detailed data sourced from the hospital. It incorporates data redundancy and data similarity and is more relevant to real-world healthcare scenarios, placing higher requirements on modeling capabilities than the former. LLaVA-Med's data is in English, while ours is in Chinese. Other commonly used datasets such as MedICaT [32], ROCO [26] and MIMIC-CXR [14] exhibit similar limitations as above.

Chinese medical chatbots. Medical assistants are emerging in the Chinese language field as well. Notably, BenTsao [38] integrates Chinese medical knowledge bases into the training and inference phases of LLMs, and thus creates a medical chatbot in Chinese language. It reflects the construction method of most prior Chinese medical chatbots [40, 43, 44, 47]. However, to the best of our knowledge, XrayGLM stands as the only existing multimodal Chinese medical chatbot capable of processing image inputs. Nevertheless, it relies on relatively coarse data and primarily focuses on chest X-rays, thus lacking data diversity. Besides, the displayed example results are mainly for images without lesions, lacking comprehensiveness. And it fails to produce more detailed answers. In contrast, our LLaVA-Ultra offers substantial enhancements in these respects.

3 Multimodal Conversational Model in the Medical Domain

3.1 Ultrasound Concept Feature Alignment

We employ a network architecture that is based on the multimodal conversation model LLaVA, incorporating a projection module to link the visual encoder with the language model. The model parameters are initialized with weights from LLaVA-Med in the English medical domain, followed by finetuning [39] using medical domain instructions derived from our Chinese ultrasound dataset. For each paired sample, given textual instructions X_q and image inputs X_v, we ask the model to produce answers X_a related to the original caption X_c, such as giving a diagnosis or describing visual contents. The instruction tuning process can be formulated as follows,

$$p(X_a|X_c, X_v, X_q) = \prod_{l=1}^{L} p_\theta(x_l|X_c, X_v, X_q, x_{1:l-1}), \quad (1)$$

加了一个投影模块连接视觉编码器和llm：adapter

LLaVA-Ultra: Large Chinese Language and Vision Assistant for Ultrasound

MM '24, October 28–November 1, 2024, Melbourne, VIC, Australia.
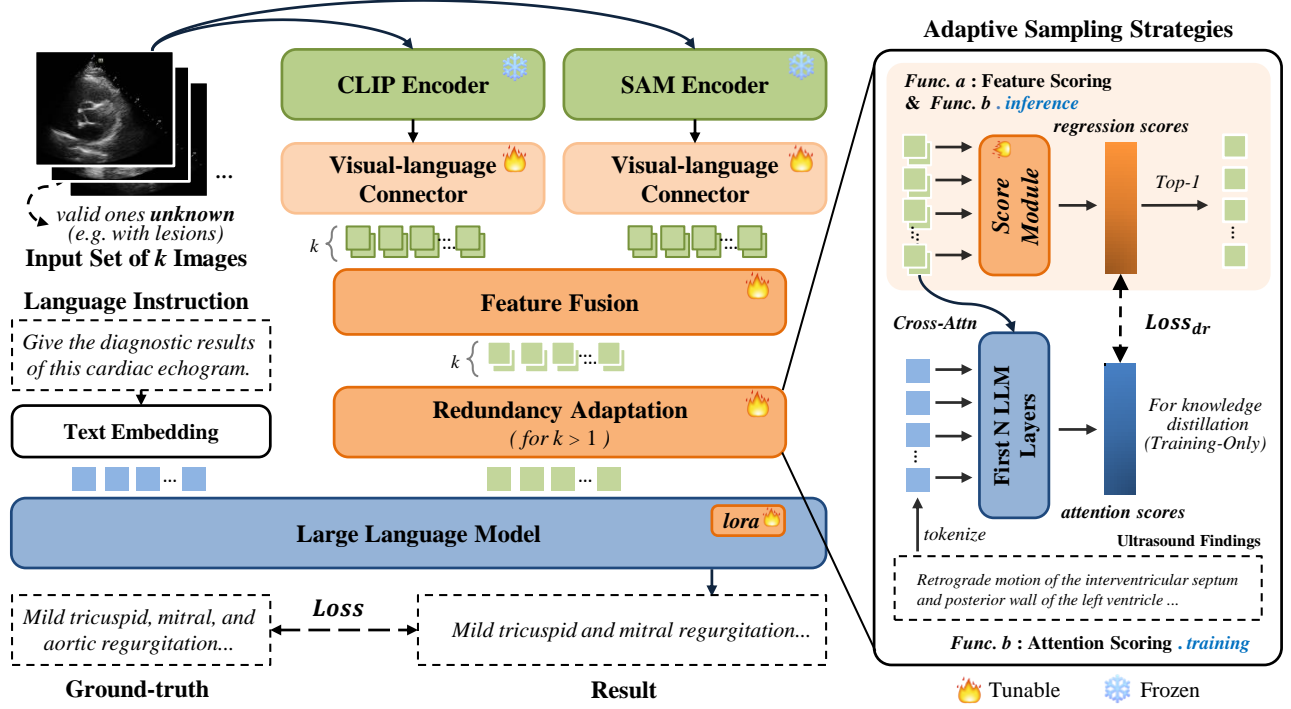

Figure 2: Overview of our proposed LLaVA-Ultra. Beyond employing the conventional MLLM's architecture, it achieves visual enhancement via a fusion module to incorporate fine-grained SAM features. Additionally, our model can adapt the data redundancy commonly occurred in medical scenarios by two designed automatic sampling strategies.

where θ is the network parameters to be optimized. Following the approach of LLaVA-Med, we conduct training in two stages. The first stage involves aligning ultrasound images with corresponding medical concepts using simple instructions. In the second stage, we utilize diverse instructions generated by GPT-3.5 [23] to enable our model to address free-form conversations. During training, we freeze the visual encoder and most of the LLM weights and update the parameters of the projection layers, LoRA [10], and our designed modules for enhancement. Through iterative optimization, the model assimilates a substantial volume of new ultrasound visual information and aligns it with medical textual concepts. As a result, it can serve as an ultrasound visual chatbot.

3.2 Visual Enhancement

Most existing MLLMs utilize the CLIP series [7, 29, 33] as visual modules, incorporating features from deep layers that represent the global context as inputs to the LLM. However, it may result in less fine-grained visual perception in MLLMs. Additionally, the improvement of MLLMs is hindered by the limitations of the visual branch [19, 30, 42], primarily due to the unbalanced scales of visual and language models (e.g. ViT-Large-300M vs. LAMA-7B/13B) [13]. Therefore, there is a need for visual enhancement in MLLMs, especially in the medical domain where image information is subtle. To address this issue, we integrate the Segment Anything Model (SAM) [16], effective in capturing finer-grained features, as an extra visual encoder and further incorporate it through a fusion strategy, as shown in Fig. 2. Specifically, the input images undergo processing

by both the CLIP and SAM (ViT-Large-based) encoders F_1, F_2 to derive visual features and then align them with the linguistic feature space of the LLM through corresponding projection modules P_{θ_1}, P_{θ_2}. We combine the resultant features H_1, H_2 using a learnable weight parameter α for feature fusion as follows,

$$H_1 = P_{\theta_1}(F_1(X_v)), H_2 = P_{\theta_2}(F_2(X_v)),$$
$$H_v = \alpha \cdot H_1 + (1 - \alpha) \cdot H_2. \tag{2}$$

It enables an appropriate balance between the two typical visual features. The fused feature H_v enriches with detailed local information, such as the texture of lesion areas. It is subsequently concatenated with the instruction tokens to serve as input for the LLM, thereby enhancing the fine-grained visual perception of the MLLM.

Discussion. (*i*) *Medical domain adaptation.* This is particularly crucial for medical images, where features like lesion areas are often more subtle compared to natural images. (*ii*) *Parameter-efficient scheme.* It validates the feasibility of visual enhancement in a parameter-efficient way for multiple frozen visual encoders. (*iii*) *Model extension.* In addition to SAM, it can be generalized to explore the application value of other vision models for MLLMs.

3.3 Adaptive Sampling for Data Redundancy

Data redundancy is commonly encountered in clinical scenes, where there is a group of images corresponding to the same text but only some images are valid. To effectively deal with this scenario while balancing computational cost, we devise an adaption module. For

MM '24, October 28–November 1, 2024, Melbourne, VIC, Australia.

Xuechen Guo, Wenhao Chai, Shi-Yan Li, & Gaoang Wang

such a paired instance, we calculate the weight scores of the grouped k images based on the features obtained from the visual-language projection. Then we sample the image with the highest score as the valid one that best matches the specifics of the text. Specifically, we design two adaptive sampling strategies, as shown in Fig. 2:

(*a*) **Feature scoring strategy.** We use the projected image feature H_v as the weight score, as the optimization of the projection modules is related to the image-text alignment during training. Since H_v contains multiple tokens h, each focusing on different content, we avoid treating them equally, such as by simply summing or averaging. Instead, we employ a set of learnable parameters w to calculate a weighted average as a score. And we sample the image with the highest score as the valid one to utilize in this group, *i.e.*,

$$s_{fea}^i = \sum_{j=1}^{d} w_j \cdot h_j,$$
$$s_{fea}^u = Sampling(\{s_{fea}^i\}), i = 1, 2, \ldots, k, \qquad (3)$$

where d is the number of channels in feature H_v. Thus, these weights can be progressively optimized during training to focus on tokens that are more expressive of the relevance of the image to the text.

(*b*) **Attention scoring strategy.** The strategy above indirectly learns to align during training. However, in our dataset, each text instance contains sufficient information to directly match the text with the most suitable image by comparing the text with each image's features. For instance, if the instruction's question pertains to the diagnosis, we can utilize the descriptive textual ultrasound findings. We leverage the first N LLM layers to perform cross attention in Visual Transformer (ViT) [6, 36] of each image feature in the paired instance and the same text of ultrasound findings H_t, *i.e.*,

$$s_{attn}^i = Attn(H_v^i, H_t), i = 1, 2, \ldots, k. \qquad (4)$$

The obtained scores directly reflect the relevance of each image to this same text. Considering the absence of additional textual knowledge during inference, we treat these attention scores as pseudo labels and calculate the cross-entropy loss with feature scores s_{fea} above after normalization, *i.e.*,

$$L_{adr} = -\sum_{i=1}^{k} Norm(s_{attn}^i) \log(Norm(s_{fea}^i)). \qquad (5)$$

By optimizing the weight parameter w with this knowledge, we can better prioritize tokens and thus screen the image that strongly correlates with the text.

Discussion. (*i*) *Fitting medical scenarios.* Our method leverages redundant medical data, which is highly relevant and practical for physicians' diagnostic processes in real-world scenarios. (*ii*) *Computational efficiency.* Instead of captioning all images corresponding to the same text and selecting the most accurate results, we offer a computationally low-cost approach. We directly select feature scores or use a small-scale attention module to screen effective images before feeding them into the LLM. Even with the employment of the redundancy adaptation module and the additional visual encoder mentioned above, it only takes 60 hours on 4 48G A40s for training. (*iii*) *Data utilization.* In the second screening method above, we leverage the textual information of ultrasound observations, a previously untapped resource. It often directly reflects

训练资源

the image's information more intuitively than diagnostic results, thus better identifying valid images. Additionally, the ultrasound observations text and the subsequent diagnostic results input into the LLM are strongly interconnected. The former serves as the surface-level description, while the latter offers a summary and in-depth characterization of the former. This intrinsic relationship facilitates the extraction of more detailed and profound medical semantics during learning. (*iv*) *Domain adaptation.* Although the focus of this paper is on the ultrasound domain, it can be generalized to other medical imaging modalities, such as CT, CXR, and MRI. There are also requirements for fine-grained analysis and cases of data redundancy in these domains. It is possible to utilize features and knowledge of these domains to construct the corresponding assistants similar to our proposed method.

4 Professional Ultrasound Multi-modal Data

4.1 Ultrasound Multi-modal Data

There is a lack of Chinese medical datasets to perform finetuning for MLLMs. To fill this gap, we present a first attempt to utilize a large-scale Chinese multimodal ultrasound hospital dataset and it has the noteworthy following characteristics that are rarely seen in previous datasets and works: (*i*) *First-hand source and diversity.* Our dataset is sourced from the hospital database. It consists of over 188k medical text descriptions paired with 1.7M ultrasound images with more than 20 examination sites, such as heart, thyroid, breast, uterus, prostate, etc. (*ii*) *Professionality.* It contains comprehensive and detailed clinical text such as examination sites, medical histories, ultrasound observations, diagnosis, etc. Professional doctors offer all the contents and thus the data reliability makes our work a valuable attempt in medical MLLM. (*iii*) *Challenges within ultrasound modality.* Imaging modalities used in previous works typically include chest X-ray (CXR), computed tomography (CT), and magnetic resonance imaging (MRI). It's relatively possible for even a layman to identify body parts (e.g. head and chest) in images of these modalities. However, such a task is difficult when confronted with ultrasound. It's more challengeable for MLLMs to learn medical semantics like a layman. (*iv*) *Fine granularity.* It contains many samples with high similarity due to the hospital source and thus places a higher requirement on fine-grained medical understanding. (*v*) *Respect for medical reality.* Datasets like PMC-15M used by LLaVA-Med typically feature paired instances where a text corresponds to a single image. However, it is often inconsistent with clinical practice where data redundancy exists. Our dataset addresses this by capturing many instances where one text is paired with multiple images from the same ultrasound video. For example, when the text describes a lesion, only images of frames scanned to the lesion are valid for mirroring the text, while those without lesion display are invalid. This challenges the model to distinguish valid images for reasoning and holds practical relevance.

4.2 Ultrasound Instruction-following Data

Inspired by LLaVA-Med, we generate Chinese ultrasound instruction-following data as Fig. 3. For one caption X_c paired with k images X_v, we create an instruction-following example with question X_q:

Human : X_q X_v^1... X_v^k<STOP>\n Assistant : X_c<STOP>\n

Ultrasound Multimodal Data Example

Examination Site:

Cardiac color Doppler ultrasound, left heart function measurement, ventricular wall motion analysis, tissue Doppler imaging

Ultrasound Observation :

EF: 67.3% AAO: 36.9 mm AO: 33.8 mm LA: 31.1 mm PA: 23.8 mm No significant abnormalities in aortic and pulmonary valve morphology, echogenicity, or activity were noted. The internal diameter of each atrium was normal. The morphology, echo, and activity of the mitral and tricuspid valves were not significantly abnormal. The interventricular septum and the posterior wall of the left ventricle showed retrograde motion. The left ventricular wall activity was not abnormal. There was no continuous interruption of the cardiac structures, and no obvious liquid dark areas were seen in the pericardial cavity.CDFI: A small amount of regurgitant signal was seen in the tricuspid, mitral, and aortic orifices.TDI: Diastolic E/A at the level of the mitral annulus was >1.0.

Diagnosis :

Mild tricuspid, mitral, and aortic regurgitation

Source: hospital
Language: Chinese

Data redundancy:
*a single **text** instance (left) paired*
*with **k images**, only some are valid*
(e.g. display lesions mentioned in text)

Visual Instruction-Following Conversations:

User: What body part is this ultrasound image from and what test is it?
Assistant: It is a cardiac color Doppler ultrasound, left heart function measurement, wall motion analysis, and tissue Doppler imaging.
User: Describe the condition of the heart in this ultrasound image.
Assistant: In this ultrasound image, all structures of the heart are normal, including the aortic valve, pulmonary valve, and mitral and tricuspid valves. The septum and posterior wall of the left ventricle are in retrograde motion, and there is no abnormal left ventricular wall motion. There were no discontinuous structures, and there were no obvious dark areas of fluid in the pericardial cavity.
User: What about the morphology and activity of the aortic and pulmonary valves?
Assistant: The morphology and activity of the aortic and pulmonary valves are within normal limits.
User: Can you describe the regurgitant signal?
Assistant: On CDFI, a small amount of regurgitant signal can be observed in the tricuspid, mitral and aortic orifices.
User: Please give a diagnosis based on this information.
Assistant: Based on the ultrasound findings, the diagnosis is mild tricuspid, mitral and aortic regurgitation.

Figure 3: An example of our GPT-3.5 [23] generated instruction-following data. Top: A professional multimodal instance from our Chinese ultrasound hospital dataset. It exists data redundancy where a text corresponds to multiple images, but only those mirroring textual descriptions are valid (e.g., display lesions mentioned in the text). Bottom: The instruction-following data generated by GPT-3.5 using the textual descriptions.

Due to the diverse types of captions and sampled questions, the instructions require answers related to examination sites, ultrasound observations, or medical diagnoses. To validate data rationality, we produce two versions of instruction data: (*i*) Our ultrasound dataset that considers examination sites as cues in questions. (*ii*) A dataset of similar size without sites mentioned in questions, while expecting the model to state it in answers. They are utilized in experiments to evaluate their impact on trained LLaVA-Ultra.

5 Experiments

5.1 Implementation Details

Datasets. Besides our large-scale hospital ultrasound dataset, we evaluate models on two open-source Med-VQA datasets, shown in Tab. 1: (*i*) **SLAKE** [20] is an English-Chinese bilingual dataset and contains 642 images and over 7000 Q&A pairs covering 12 diseases and 39 organs, with CT, MRI, and X-Ray imaging modalities. The Q&As span various topics such as diagnosis, anatomical structure, and lesion location. Presently, SLAKE serves as a crucial benchmark for VQA tasks in the medical domain for its diversity. It has been utilized for evaluation purposes in significant medical multimodal large language model works, such as LLaVA-Med, Med PaLM M,

and PMC-VQA. (*ii*) **OpenI** [5, 12] is a chest radiograph dataset from Indiana University Hospital. XrayGLM [40] has preprocessed these unstructured data and translated the English reports into Chinese using ChatGPT. This can provide support in the case of insufficient open-source Chinese multimodal medical data. Our experiments adopt this obtained set comprising 6,436 images and 3,218 reports.

Evaluation Metrics. Based on LLaVA-Med's evaluation metrics, we've made further improvements. We tokenize model-generated answers and ground-truth separately, then calculate metrics. For open-set questions, we report the Exact Match (EM) score, F1 score, Precision, Recall and Bilingual Evaluation Understudy (BLEU) score [25]. Notably, BLEU score utilizes precise matching of 4-grams of sequences to evaluate text generation results. We adjust the weights of n-grams and obtain the scores with 1-gram, 2-gram, 3-gram and the uniform set for comprehensive evaluation in accuracy and fluency. In SLAKE, we extra report LLaVA-Ultra's results in CT, MRI, and X-Ray subsets and utilize accuracy scores for the closed-set.

Experiment Details. LLaVA-Ultra is initialized with weights from LLaVA-Med in modules included in the latter. It utilizes CLIP-ViT-L/14 and extra SAM-ViT-L as visual encoders and LLaMA-13B as LLM. We use the linear projection for multimodal connection.

Table 1: Datasets for evaluation. For the bilingual dataset, the content of both language versions is essentially identical. Therefore, we present only the data attributes of the Chinese version here.

	US-Hospital			SLAKE			OpenI		
Image Modality	Ultrasound			CT, MRI, X-Ray			Chest X-Ray		
Subset	Train	Val	Test	Train	Val	Test	Train	Val	Test
Q&A Pairs	353690	11516	11346	5967	607	491	5836	200	400
Images	1604673	49994	49996	542	50	50	5836	200	400
Text	176845	5758	5673	5967	607	491	2918	100	200
Average Word Length	133			3			90		
Open / Closed	✓ / ✗			✓ / ✓			✓ / ✗		
CHN / EN	✓ / ✗			✓ / ✓			✓ / ✓		

Table 2: Quantitative comparisons with prior SOTA methods fine-tuned on relevant datasets. Our model performs best or equal in the Chinese cases, demonstrating its effectiveness and robustness. Its results are acceptable in the English cases that are not included in our Chinese-only pre-training. It indicates the knowledge of our LLM at initialization is not significantly corrupted.

				Open-Set					Closed-Set
Method	EM	F1	Precision	Recall	BLEU	BLEU-1	BLEU- 2	BLEU-3	Accuracy
on US-Hospital Chinese dataset									
LLaVA	59.50	66.97	76.65	64.78	39.50	48.29	42.30	38.83	-
LLaVA-Med	50.55	70.77	73.91	**73.42**	40.42	50.32	43.23	39.36	-
LLaVA-Ultra	**62.00**	**72.17**	**78.84**	72.67	**48.62**	**57.71**	**51.51**	**47.95**	-
on SLAKE-zh dataset									
LLaVA	72.56	75.36	76.76	76.00	44.85	70.43	62.43	53.28	65.29
LLaVA-Med	75.02	**77.08**	78.98	**77.07**	49.31	72.61	65.09	56.96	73.58
LLaVA-Ultra (CT)	83.34	68.96	77.13	65.39	40.91	68.49	61.58	50.54	74.50
LLaVA-Ultra (MRI)	93.39	81.18	84.64	77.36	55.07	86.99	82.09	72.23	75.16
LLaVA-Ultra (X-Ray)	90.53	80.54	83.97	76.83	65.19	86.97	79.82	72.09	83.84
LLaVA-Ultra (All modalities)	**88.99**	76.85	**81.88**	73.15	**53.95**	**80.76**	**74.39**	**64.90**	**76.77**
on SLAKE-en dataset									
LLaVA	76.75	75.83	77.20	75.99	15.47	72.95	61.18	37.54	65.50
LLaVA-Med	78.22	**77.55**	**78.61**	**78.01**	**18.12**	**74.77**	**62.65**	**39.67**	65.50
LLaVA-Ultra (CT)	77.57	69.09	71.87	68.61	19.26	71.21	53.07	30.02	51.43
LLaVA-Ultra (MRI)	73.60	60.80	67.44	58.15	8.18	58.93	37.35	15.93	64.34
LLaVA-Ultra (X-Ray)	94.67	80.07	87.21	77.10	19.66	80.57	70.06	43.99	86.27
LLaVA-Ultra (All modalities)	**81.33**	68.69	74.82	66.31	13.95	68.31	51.02	27.77	**67.25**
on OpenI-zh dataset									
LLaVA	37.36	72.90	76.78	71.06	25.36	48.29	28.42	20.62	-
LLaVA-Med	35.13	**74.73**	79.26	**71.96**	27.10	50.60	30.44	22.10	-
LLaVA-Ultra	**49.32**	72.71	**82.83**	70.43	**29.37**	**51.81**	**32.61**	**24.40**	-
on OpenI-en dataset									
LLaVA	41.63	56.36	61.58	54.24	17.50	39.45	21.77	13.67	-
LLaVA-Med	**46.78**	**57.23**	**63.44**	54.10	**18.50**	39.85	22.54	**14.65**	-
LLaVA-Ultra	41.90	56.75	61.10	**55.16**	18.49	**40.31**	**22.67**	14.56	-

To ensure fair comparisons, we maintain parameters of compared models in accordance with the respective papers or codes and train until loss functions converge. Data preprocessing ways are also the same. Experiments employ 4 48GB NVIDIA A40s with PyTorch. We optimize models by Adam [15] with learning rate $1e^{-3}$.

5.2 Performance and Comparisons

We provide the comparisons between LLaVA, LLaVA-Med, and our LLaVA-Ultra when employed as a medical visual chatbot.

For qualitative comparisons shown in Fig. 4, LLaVA model for the general domain struggles with medical tasks, highlighting the gap between domains. While tailored for the medical domain, LLaVA-Med still inadequately addresses Chinese ultrasound scenes. It often focuses solely on textual medical concepts in the questions and offers vague and invalid answers that do not meet the questioner's needs. They tend to rely more on medical knowledge learned early from the LLMs rather than effectively incorporating medical visual features. This results in responses that display weak correlations
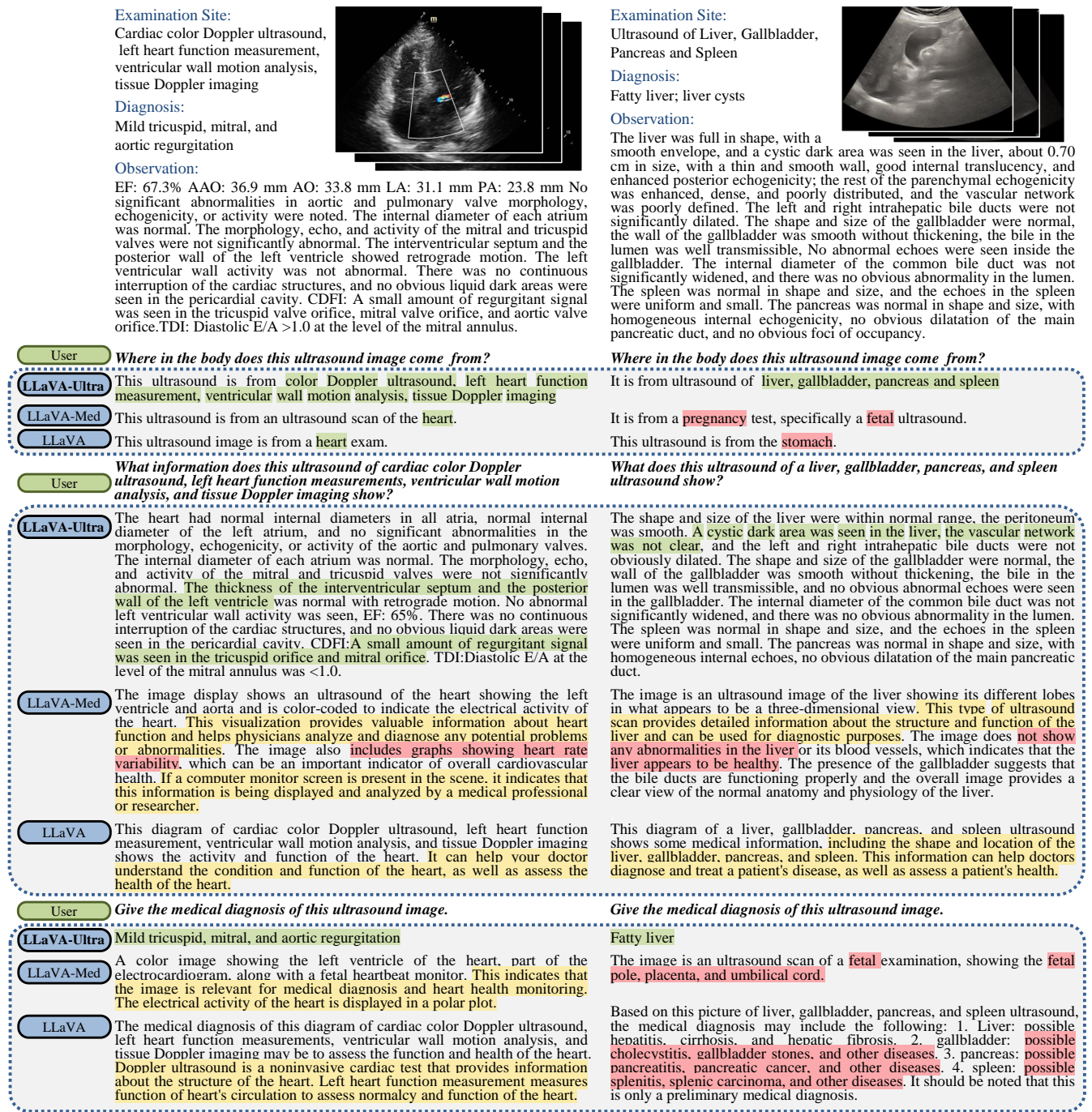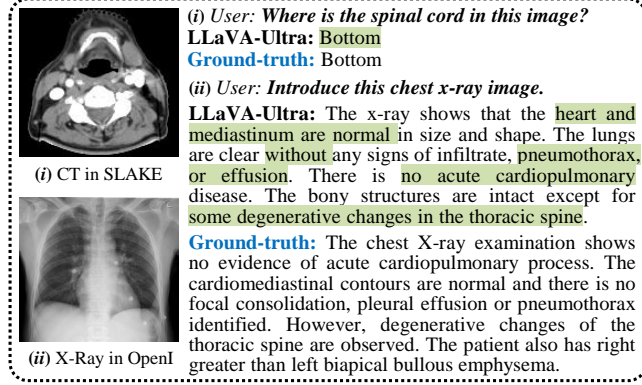
LLaVA-Ultra: Large Chinese Language and Vision Assistant for Ultrasound

MM '24, October 28–November 1, 2024, Melbourne, VIC, Australia.

Examination Site:
Cardiac color Doppler ultrasound, left heart function measurement, ventricular wall motion analysis, tissue Doppler imaging

Diagnosis:
Mild tricuspid, mitral, and aortic regurgitation

Observation:
EF: 67.3% AAO: 36.9 mm AO: 33.8 mm LA: 31.1 mm PA: 23.8 mm No significant abnormalities in aortic and pulmonary valve morphology, echogenicity, or activity were noted. The internal diameter of each atrium was normal. The morphology, echo, and activity of the mitral and tricuspid valves were not significantly abnormal. The interventricular septum and the posterior wall of the left ventricle showed retrograde motion. The left ventricular wall activity was not abnormal. There was no continuous interruption of the cardiac structures, and no obvious liquid dark areas were seen in the pericardial cavity. CDFI: A small amount of regurgitant signal was seen in the tricuspid valve orifice, mitral valve orifice, and aortic valve orifice. TDI: Diastolic E/A >1.0 at the level of the mitral annulus.

Examination Site:
Ultrasound of Liver, Gallbladder, Pancreas and Spleen

Diagnosis:
Fatty liver; liver cysts

Observation:
The liver was full in shape, with a smooth envelope, and a cystic dark area was seen in the liver, about 0.70 cm in size, with a thin and smooth wall, good internal translucency, and enhanced posterior echogenicity; the rest of the parenchymal echogenicity was enhanced, dense, and poorly distributed, and the vascular network was poorly defined. The left and right intrahepatic bile ducts were not significantly dilated. The shape and size of the gallbladder were normal, the wall of the gallbladder was smooth without thickening, the bile in the lumen was well transmissible, No abnormal echoes were seen inside the gallbladder. The internal diameter of the common bile duct was not significantly widened, and there was no obvious abnormality in the lumen. The spleen was normal in shape and size, and the echoes in the spleen were uniform and small. The pancreas was normal in shape and size, with homogeneous internal echogenicity, no obvious dilatation of the main pancreatic duct, and no obvious foci of occupancy.

User — *Where in the body does this ultrasound image come from?*

LLaVA-Ultra — This ultrasound is from color Doppler ultrasound, left heart function measurement, ventricular wall motion analysis, tissue Doppler imaging

LLaVA-Med — This ultrasound is from an ultrasound scan of the heart.

LLaVA — This ultrasound image is from a heart exam.

User — *Where in the body does this ultrasound image come from?*

LLaVA-Ultra — It is from ultrasound of liver, gallbladder, pancreas and spleen

LLaVA-Med — It is from a pregnancy test, specifically a fetal ultrasound.

LLaVA — This ultrasound is from the stomach.

User — *What information does this ultrasound of cardiac color Doppler ultrasound, left heart function measurements, ventricular wall motion analysis, and tissue Doppler imaging show?*

LLaVA-Ultra — The heart had normal internal diameters in all atria, normal internal diameter of the left atrium, and no significant abnormalities in the morphology, echogenicity, or activity of the aortic and pulmonary valves. The internal diameter of each atrium was normal. The morphology, echo, and activity of the mitral and tricuspid valves were not significantly abnormal. The thickness of the interventricular septum and the posterior wall of the left ventricle was normal with retrograde motion. No abnormal left ventricular wall activity was seen, EF: 65%. There was no continuous interruption of the cardiac structures, and no obvious liquid dark areas were seen in the pericardial cavity. CDFI: A small amount of regurgitant signal was seen in the tricuspid orifice and mitral orifice. TDI: Diastolic E/A at the level of the mitral annulus was <1.0.

LLaVA-Med — The image display shows an ultrasound of the heart showing the left ventricle and aorta and is color-coded to indicate the electrical activity of the heart. This visualization provides valuable information about heart function and helps physicians analyze and diagnose any potential problems or abnormalities. The image also includes graphs showing heart rate variability, which can be an important indicator of overall cardiovascular health. If a computer monitor screen is present in the scene, it indicates that this information is being displayed and analyzed by a medical professional or researcher.

LLaVA — This diagram of cardiac color Doppler ultrasound, left heart function measurement, ventricular wall motion analysis, and tissue Doppler imaging shows the activity and function of the heart. It can help your doctor understand the condition and function of the heart, as well as assess the health of the heart.

User — *What does this ultrasound of a liver, gallbladder, pancreas, and spleen ultrasound show?*

LLaVA-Ultra — The shape and size of the liver were within normal range, the peritoneum was smooth. A cystic dark area was seen in the liver, the vascular network was not clear, and the left and right intrahepatic bile ducts were not obviously dilated. The shape and size of the gallbladder were normal, the wall of the gallbladder was smooth without thickening, the bile in the lumen was well transmissible, and no obvious abnormal echoes were seen in the gallbladder. The internal diameter of the common bile duct was not significantly widened, and there was no obvious abnormality in the lumen. The spleen was normal in shape and size, and the echoes in the spleen were uniform and small. The pancreas was normal in shape and size, with homogeneous internal echoes, no obvious dilatation of the main pancreatic duct.

LLaVA-Med — The image is an ultrasound image of the liver showing its different lobes in what appears to be a three-dimensional view. This type of ultrasound scan provides detailed information about the structure and function of the liver and can be used for diagnostic purposes. The image does not show any abnormalities in the liver or its blood vessels, which indicates that the liver appears to be healthy. The presence of the gallbladder suggests that the bile ducts are functioning properly and the overall image provides a clear view of the normal anatomy and physiology of the liver.

LLaVA — This diagram of a liver, gallbladder, pancreas, and spleen ultrasound shows some medical information, including the shape and location of the liver, gallbladder, pancreas, and spleen. This information can help doctors diagnose and treat a patient's disease, as well as assess a patient's health.

User — *Give the medical diagnosis of this ultrasound image.*

LLaVA-Ultra — Mild tricuspid, mitral, and aortic regurgitation

LLaVA-Med — A color image showing the left ventricle of the heart, part of the electrocardiogram, along with a fetal heartbeat monitor. This indicates that the image is relevant for medical diagnosis and heart health monitoring. The electrical activity of the heart is displayed in a polar plot.

LLaVA — The medical diagnosis of this diagram of cardiac color Doppler ultrasound, left heart function measurements, ventricular wall motion analysis, and tissue Doppler imaging may be to assess the function and health of the heart. Doppler ultrasound is a noninvasive cardiac test that provides information about the structure of the heart. Left heart function measurement measures function of heart's circulation to assess normalcy and function of the heart.

User — *Give the medical diagnosis of this ultrasound image.*

LLaVA-Ultra — Fatty liver

LLaVA-Med — The image is an ultrasound scan of a fetal examination, showing the fetal pole, placenta, and umbilical cord.

LLaVA — Based on this picture of liver, gallbladder, pancreas, and spleen ultrasound, the medical diagnosis may include the following: 1. Liver: possible hepatitis, cirrhosis, and hepatic fibrosis. 2. gallbladder: possible cholecystitis, gallbladder stones, and other diseases. 3. pancreas: possible pancreatitis, pancreatic cancer, and other diseases. 4. spleen: possible splenitis, splenic carcinoma, and other diseases. It should be noted that this is only a preliminary medical diagnosis.

Figure 4: Comparisons in medical visual conversations. LLaVA and LLaVA-Med tend to give vague answers irrelevant to images and wrong results. In contrast, LLaVA-Ultra offers more correct and specific responses associated with visual contents.

with the input images and even exhibit inaccuracy. It implies the flaws in their model structures. In contrast, our LLaVA-Ultra model delivers more correct and specific answers closely aligned with the visual content of the input medical image. This notable performance demonstrates the capability of LLaVA-Ultra.

Table. 2 further presents the quantitative comparison results. We finetune LLaVA and LLaVA-Med on the training set of our Chinese ultrasound hospital dataset and report their metrics on the test set. For SLAKE and OpenI, we finetune and evaluate all three models. The results clearly show that LLaVA-Ultra outperforms

Table 3: Ablation study: several variants of our model structure on US-Hospital Chinese dataset.

Variant	EM	F1	Precision	Recall	BLEU	BLEU-1	BLEU-2	BLEU-3
w/o. Visual enhancement	57.01	71.37	75.23	72.11	45.81	55.96	49.15	45.12
w/o. Redundancy adaption	50.13	70.57	72.37	**73.91**	41.03	51.57	44.24	40.08
w/o. Func.b redundancy adaption	51.86	70.95	73.75	73.84	41.52	51.09	44.21	40.39
w/o. Stage 2 tuning	54.52	71.36	75.83	72.45	43.54	53.19	46.36	42.59
w/o. Site prompt in instruction	57.48	71.57	76.84	71.63	45.13	54.61	48.03	44.31
LLaVA-Ultra full model	**62.00**	**72.17**	**78.84**	72.67	**48.62**	**57.71**	**51.51**	**47.95**

*(i) User: **Where is the spinal cord in this image?***
LLaVA-Ultra: Bottom
Ground-truth: Bottom

*(ii) User: **Introduce this chest x-ray image.***
LLaVA-Ultra: The x-ray shows that the heart and mediastinum are normal in size and shape. The lungs are clear without any signs of infiltrate, pneumothorax, or effusion. There is no acute cardiopulmonary disease. The bony structures are intact except for some degenerative changes in the thoracic spine.
Ground-truth: The chest X-ray examination shows no evidence of acute cardiopulmonary process. The cardiomediastinal contours are normal and there is no focal consolidation, pleural effusion or pneumothorax identified. However, degenerative changes of the thoracic spine are observed. The patient also has right greater than left biapical bullous emphysema.

(i) CT in SLAKE
(ii) X-Ray in OpenI

Figure 5: Case study: downstream English tasks reveals Chinese pretrain does not visibly damage early LLM knowledge.

both LLaVA and LLaVA-Med on our Chinese ultrasound dataset. It proves the superiority of our model architecture, particularly the visual enhancement and redundancy adaptation modules. When evaluated on the downstream tasks of Chinese language in SLAKE and OpenI, LLaVA-Ultra consistently delivers the best performance across open-set and close-set questions, which demonstrates its robustness. This suggests that our model effectively learns to map medical semantics to correct features during training. Even on English data subsets, LLaVA-Ultra offers acceptable results shown in Table. 2 and Fig. 5, which may benefit from its textual knowledge acquired during LLM initialization. This indicates that its training on the Chinese dataset does not significantly compromise this part of English knowledge [46]. We also report results in CT, MRI, and X-Ray subsets on SLAKE besides the overall average values. Our model pretrained on ultrasound modality shows effective adaptability across diverse imaging modalities. It highlights LLaVA-Ultra's robustness and versatility in accomplishing downstream multimodal tasks after simple finetuning.

5.3 Ablation Study

To assess the validity of the model's components, we conducted comparative experiments on several aspects shown in Tab. 3.

Visual enhancement. To prove the necessity of visual enhancement, we replace our dual visual encoders and its fusion module with the original single CLIP encoder and observe the decrease of all metrics in Tab. 3. This verifies the necessity of strengthening the visual branch of MLLMs and underlines the effectiveness of our feature fusion strategy. The integration of SAM features enables

LLaVA-Ultra to extract finer-grained visual semantics, which is a crucial aspect of handling subtle information in medical scenarios.

Data redundancy adaptation. We remove our data redundancy adaptation module, the metrics in Table. 3 show a significant reduction. This highlights the importance of addressing data redundancy, which is prevalent in real medical scenarios but less noticed. In previous works, when multiple images correspond to the same text, such text is often assigned to each image. It results in mapping the images that don't mirror the specific text, i.e. redundant data, and the valid images to a similar feature representation. This hinders the model from learning accurate medical semantics and cross-modal alignment. As shown in the scores, LLaVA-Ultra full model can address this issue effectively with our adaption strategy. Specifically, our attention scoring strategy (Func.b) leverages rich textual data for feature alignment and thus achieves better scores compared to the simpler feature scoring (Func.a).

Data construction. We modified the instruction data by removing the cues of the examination site from the question. Instead, we ask a generalized question like *"give the diagnosis of this ultrasound image"*. Results in Tab. 3 indicate a slight decrease in evaluation metrics within acceptable limits. This demonstrates the effectiveness of limited cues for the model to learn specific medical knowledge, as well as the robustness of our model structure.

5.4 Limitation

Although LLaVA-Ultra shows impressive capabilities in Chinese medical multimodal understanding, it still has some limitations, including: 1) Its performance is hindered by the scale of the pretrained vision models. 2) Our large-scale medical dataset has not yet included more comprehensive labels e.g., segmentation to allow our model to engage further enhancement in visual perception.

6 Conclusion

We propose LLaVA-Ultra, a large Chinese language and vision assistant for the ultrasound domain. To achieve this, we create a high-quality visual-language instruction-following dataset from the large-scale professional ultrasound database of hospitals. More importantly, we improve the conventional visual language model structure by performing visual enhancement and data redundancy adaptation. It enables LLaVA-Ultra to fit the needs of fine-grained medical information and practical clinical scenarios, thus producing high-quality responses in medical visual conversations. On three medical VQA datasets, LLaVA-Ultra outperforms previous SOTA in various metrics, demonstrating its effectiveness and robustness.

LLaVA-Ultra: Large Chinese Language and Vision Assistant for Ultrasound

MM '24, October 28–November 1, 2024, Melbourne, VIC, Australia.

Acknowledgments

References

[1] Keqin Chen, Zhao Zhang, Weili Zeng, Richong Zhang, Feng Zhu, and Rui Zhao. 2023. Shikra: Unleashing Multimodal LLM's Referential Dialogue Magic. arXiv:2306.15195 [cs.CV]

[2] Shaoxiang Chen, Zequn Jie, and Lin Ma. 2024. LLaVA-MoLE: Sparse Mixture of LoRA Experts for Mitigating Data Conflicts in Instruction Finetuning MLLMs. arXiv:2401.16160 [cs.CV]

[3] Wei-Lin Chiang, Zhuohan Li, Zi Lin, Ying Sheng, Zhanghao Wu, Hao Zhang, Lianmin Zheng, Siyuan Zhuang, Yonghao Zhuang, Joseph E. Gonzalez, Ion Stoica, and Eric P. Xing. 2023. Vicuna: An Open-Source Chatbot Impressing GPT-4 with 90%* ChatGPT Quality. https://lmsys.org/blog/2023-03-30-vicuna/

[4] Xiangxiang Chu, Limeng Qiao, Xinyang Lin, Shuang Xu, Yang Yang, Yiming Hu, Fei Wei, Xinyu Zhang, Bo Zhang, Xiaolin Wei, and Chunhua Shen. 2023. MobileVLM : A Fast, Strong and Open Vision Language Assistant for Mobile Devices. arXiv:2312.16886 [cs.CV]

[5] Dina Demner-Fushman, Marc Kohli, Marc Rosenman, Sonya Shooshan, Laritza Rodriguez, Sameer Antani, George Thoma, and Clement Mcdonald. 2015. Preparing a collection of radiology examinations for distribution and retrieval. *Journal of the American Medical Informatics Association : JAMIA* 23 (07 2015). https://doi.org/10.1093/jamia/ocv080

[6] Alexey Dosovitskiy, Lucas Beyer, Alexander Kolesnikov, Dirk Weissenborn, Xiaohua Zhai, Thomas Unterthiner, Mostafa Dehghani, Matthias Minderer, Georg Heigold, Sylvain Gelly, Jakob Uszkoreit, and Neil Houlsby. 2021. An Image is Worth 16x16 Words: Transformers for Image Recognition at Scale. arXiv:2010.11929 [cs.CV]

[7] Sedigheh Eslami, Gerard de Melo, and Christoph Meinel. 2021. Does CLIP Benefit Visual Question Answering in the Medical Domain as Much as it Does in the General Domain? arXiv:2112.13906 [cs.CV]

[8] Chaoyou Fu, Peixian Chen, Yunhang Shen, Yulei Qin, Mengdan Zhang, Xu Lin, Jinrui Yang, Xiawu Zheng, Ke Li, Xing Sun, Yunsheng Wu, and Rongrong Ji. 2024. MME: A Comprehensive Evaluation Benchmark for Multimodal Large Language Models. arXiv:2306.13394 [cs.CV]

[9] Chaoyou Fu, Renrui Zhang, Zihan Wang, Yubo Huang, Zhengye Zhang, Longtian Qiu, Gaoxiang Ye, Yunhang Shen, Mengdan Zhang, Peixian Chen, Sirui Zhao, Shaohui Lin, Deqiang Jiang, Di Yin, Peng Gao, Ke Li, Hongsheng Li, and Xing Sun. 2023. A Challenger to GPT-4V? Early Explorations of Gemini in Visual Expertise. arXiv:2312.12436 [cs.CV]

[10] Edward J. Hu, Yelong Shen, Phillip Wallis, Zeyuan Allen-Zhu, Yuanzhi Li, Shean Wang, Lu Wang, and Weizhu Chen. 2021. LoRA: Low-Rank Adaptation of Large Language Models. arXiv:2106.09685 [cs.CL]

[11] Shaohan Huang, Li Dong, Wenhui Wang, Yaru Hao, Saksham Singhal, Shuming Ma, Tengchao Lv, Lei Cui, Owais Khan Mohammed, Barun Patra, Qiang Liu, Kriti Aggarwal, Zewen Chi, Johan Bjorck, Vishrav Chaudhary, Subhojit Som, Xia Song, and Furu Wei. 2023. Language Is Not All You Need: Aligning Perception with Language Models. arXiv:2302.14045 [cs.CL]

[12] Stefan Jaeger, Sema Candemir, Sameer Antani, Yì-Xiáng Wáng, Pu-Xuan Lu, and George Thoma. 2014. Two public chest X-ray datasets for computer-aided screening of pulmonary diseases. *Quantitative imaging in medicine and surgery* 4 (12 2014), 475–7. https://doi.org/10.3978/j.issn.2223-4292.2014.11.20

[13] Dongsheng Jiang, Yuchen Liu, Songlin Liu, Jin'e Zhao, Hao Zhang, Zhen Gao, Xiaopeng Zhang, Jin Li, and Hongkai Xiong. 2024. From CLIP to DINO: Visual Encoders Shout in Multi-modal Large Language Models. arXiv:2310.08825 [cs.CV]

[14] Alistair E. W. Johnson, Tom J. Pollard, Nathaniel R. Greenbaum, Matthew P. Lungren, Chih ying Deng, Yifan Peng, Zhiyong Lu, Roger G. Mark, Seth J. Berkowitz, and Steven Horng. 2019. MIMIC-CXR-JPG, a large publicly available database of labeled chest radiographs. arXiv:1901.07042 [cs.CV]

[15] Diederik P. Kingma and Jimmy Ba. 2017. Adam: A Method for Stochastic Optimization. arXiv:1412.6980 [cs.LG]

[16] Alexander Kirillov, Eric Mintun, Nikhila Ravi, Hanzi Mao, Chloe Rolland, Laura Gustafson, Tete Xiao, Spencer Whitehead, Alexander C. Berg, Wan-Yen Lo, Piotr Dollár, and Ross Girshick. 2023. Segment Anything. arXiv:2304.02643 [cs.CV]

[17] Chunyuan Li, Cliff Wong, Sheng Zhang, Naoto Usuyama, Haotian Liu, Jianwei Yang, Tristan Naumann, Hoifung Poon, and Jianfeng Gao. 2023. LLaVA-Med: Training a Large Language-and-Vision Assistant for Biomedicine in One Day. arXiv:2306.00890 [cs.CV]

[18] Junnan Li, Dongxu Li, Silvio Savarese, and Steven Hoi. 2023. BLIP-2: Bootstrapping Language-Image Pre-training with Frozen Image Encoders and Large Language Models. arXiv:2301.12597 [cs.CV]

[19] Zhang Li, Biao Yang, Qiang Liu, Zhiyin Ma, Shuo Zhang, Jingxu Yang, Yabo Sun, Yuliang Liu, and Xiang Bai. 2024. Monkey: Image Resolution and Text Label Are Important Things for Large Multi-modal Models. arXiv:2311.06607 [cs.CV]

[20] Bo Liu, Li-Ming Zhan, Li Xu, Lin Ma, Yan Yang, and Xiao-Ming Wu. 2021. SLAKE: A Semantically-Labeled Knowledge-Enhanced Dataset for Medical Visual Question Answering. arXiv:2102.09542 [cs.CV]

[21] Haotian Liu, Chunyuan Li, Qingyang Wu, and Yong Jae Lee. 2023. Visual Instruction Tuning. arXiv:2304.08485 [cs.CV]

[22] Jiasen Lu, Christopher Clark, Sangho Lee, Zichen Zhang, Savya Khosla, Ryan Marten, Derek Hoiem, and Aniruddha Kembhavi. 2023. Unified-IO 2: Scaling Autoregressive Multimodal Models with Vision, Language, Audio, and Action. arXiv:2312.17172 [cs.CV]

[23] OpenAI. 2022. ChatGPT. https://openai.com/blog/chatgpt/.

[24] OpenAI. 2023. GPT-4 Technical Report. https://arxiv.org/abs/2303.08774. arXiv:2303.08774 [cs.CL]

[25] Kishore Papineni, Salim Roukos, Todd Ward, and Wei Jing Zhu. 2002. BLEU: a Method for Automatic Evaluation of Machine Translation. (10 2002). https://doi.org/10.3115/1073083.1073135

[26] Obioma Pelka, Sven Koitka, Johannes Rückert, Felix Nensa, and Christoph M. Friedrich. 2018. Radiology Objects in COntext (ROCO): A Multimodal Image Dataset. In *Intravascular Imaging and Computer Assisted Stenting and Large-Scale Annotation of Biomedical Data and Expert Label Synthesis*, Danail Stoyanov, Zeike Taylor, Simone Balocco, Raphael Sznitman, Anne Martel, Lena Maier-Hein, Luc Duong, Guillaume Zahnd, Stefanie Demirci, Shadi Albarqouni, Su-Lin Lee, Stefano Moriconi, Veronika Cheplygina, Diana Mateus, Emanuele Trucco, Eric Granger, and Pierre Jannin (Eds.). Springer International Publishing, Cham, 180–189.

[27] Baolin Peng, Chunyuan Li, Pengcheng He, Michel Galley, and Jianfeng Gao. 2023. Instruction Tuning with GPT-4. arXiv:2304.03277 [cs.CL]

[28] Jianing Qiu, Lin Li, Jiankai Sun, Jiachuan Peng, Peilun Shi, Ruiyang Zhang, Yinzhao Dong, Kyle Lam, Frank P.-W. Lo, Bo Xiao, Wu Yuan, Ningli Wang, Dong Xu, and Benny Lo. 2023. Large AI Models in Health Informatics: Applications, Challenges, and the Future. *IEEE Journal of Biomedical and Health Informatics* 27, 12 (Dec. 2023), 6074–6087. https://doi.org/10.1109/jbhi.2023.3316750

[29] Alec Radford, Jong Wook Kim, Chris Hallacy, Aditya Ramesh, Gabriel Goh, Sandhini Agarwal, Girish Sastry, Amanda Askell, Pamela Mishkin, Jack Clark, Gretchen Krueger, and Ilya Sutskever. 2021. Learning Transferable Visual Models From Natural Language Supervision. arXiv:2103.00020 [cs.CV]

[30] Yunhang Shen, Chaoyou Fu, Peixian Chen, Mengdan Zhang, Ke Li, Xing Sun, Yunsheng Wu, Shaohui Lin, and Rongrong Ji. 2023. Aligning and Prompting Everything All at Once for Universal Visual Perception. arXiv:2312.02153 [cs.CV]

[31] Enxin Song, Wenhao Chai, Guanhong Wang, Yucheng Zhang, Haoyang Zhou, Feiyang Wu, Xun Guo, Tian Ye, Yan Lu, Jenq-Neng Hwang, et al. 2023. Moviechat: From dense token to sparse memory for long video understanding. *arXiv preprint arXiv:2307.16449* (2023).

[32] Sanjay Subramanian, Lucy Lu Wang, Sachin Mehta, Ben Bogin, Madeleine van Zuylen, Sravanthi Parasa, Sameer Singh, Matt Gardner, and Hannaneh Hajishirzi. 2020. MedICaT: A Dataset of Medical Images, Captions, and Textual References. arXiv:2010.06000 [cs.CV]

[33] Zeyi Sun, Ye Fang, Tong Wu, Pan Zhang, Yuhang Zang, Shu Kong, Yuanjun Xiong, Dahua Lin, and Jiaqi Wang. 2023. Alpha-CLIP: A CLIP Model Focusing on Wherever You Want. arXiv:2312.03818 [cs.CV]

[34] Hugo Touvron, Thibaut Lavril, Gautier Izacard, Xavier Martinet, Marie-Anne Lachaux, Timothée Lacroix, Baptiste Rozière, Naman Goyal, Eric Hambro, Faisal Azhar, Aurelien Rodriguez, Armand Joulin, Edouard Grave, and Guillaume Lample. 2023. LLaMA: Open and Efficient Foundation Language Models. arXiv:2302.13971 [cs.CL]

[35] Tao Tu, Shekoofeh Azizi, Danny Driess, Mike Schaekermann, Mohamed Amin, Pi-Chuan Chang, Andrew Carroll, Chuck Lau, Ryutaro Tanno, Ira Ktena, Basil Mustafa, Aakanksha Chowdhery, Yun Liu, Simon Kornblith, David Fleet, Philip Mansfield, Sushant Prakash, Renee Wong, Sunny Virmani, Christopher Semturs, S Sara Mahdavi, Bradley Green, Ewa Dominowska, Blaise Aguera y Arcas, Joelle Barral, Dale Webster, Greg S. Corrado, Yossi Matias, Karan Singhal, Pete Florence, Alan Karthikesalingam, and Vivek Natarajan. 2023. Towards Generalist Biomedical AI. arXiv:2307.14334 [cs.CL]

[36] Ashish Vaswani, Noam Shazeer, Niki Parmar, Jakob Uszkoreit, Llion Jones, Aidan N. Gomez, Lukasz Kaiser, and Illia Polosukhin. 2023. Attention Is All You Need. arXiv:1706.03762 [cs.CL]

[37] Chenyu Wang, Weixin Luo, Qianyu Chen, Haonan Mai, Jindi Guo, Sixun Dong, Xiaohua, Xuan, Zhengxin Li, Lin Ma, and Shenghua Gao. 2024. MLLM-Tool: A Multimodal Large Language Model For Tool Agent Learning. arXiv:2401.10727 [cs.CV]

[38] Haochun Wang, Chi Liu, Nuwa Xi, Zewen Qiang, Sendong Zhao, Bing Qin, and Ting Liu. 2023. HuaTuo: Tuning LLaMA Model with Chinese Medical Knowledge. arXiv:2304.06975 [cs.CL]

[39] Haixin Wang, Xinlong Yang, Jianlong Chang, Dian Jin, Jinan Sun, Shikun Zhang, Xiao Luo, and Qi Tian. 2023. Parameter-efficient Tuning of Large-scale Multimodal Foundation Model. arXiv:2305.08381 [cs.CV]

[40] Rongsheng Wang, Yaofei Duan, Junrong Li, Patrick Pang, and Tao Tan. 2023. XrayGLM: The first Chinese Medical Multimodal Model that Chest Radiographs Summarization. https://github.com/WangRongsheng/XrayGLM.

[41] Fei Wei, Xinyu Zhang, Ailing Zhang, Bo Zhang, and Xiangxiang Chu. 2023. Lenna: Language Enhanced Reasoning Detection Assistant. arXiv:2312.02433 [cs.CV]

[42] Penghao Wu and Saining Xie. 2023. V*: Guided Visual Search as a Core Mechanism in Multimodal LLMs. arXiv:2312.14135 [cs.CV]

[43] Honglin Xiong, Sheng Wang, Yitao Zhu, Zihao Zhao, Yuxiao Liu, Qian Wang, and Dinggang Shen. 2023. Doctorglm: Fine-tuning your chinese doctor is not a herculean task. *arXiv preprint arXiv:2304.01097* (2023).

[44] Ming Xu. 2023. MedicalGPT: Training Medical GPT Model. https://github.com/shibing624/MedicalGPT.

[45] Shukang Yin, Chaoyou Fu, Sirui Zhao, Ke Li, Xing Sun, Tong Xu, and Enhong Chen. 2023. A Survey on Multimodal Large Language Models. arXiv:2306.13549 [cs.CV]

[46] Yuexiang Zhai, Shengbang Tong, Xiao Li, Mu Cai, Qing Qu, Yong Jae Lee, and Yi Ma. 2023. Investigating the Catastrophic Forgetting in Multimodal Large Language Models. arXiv:2309.10313 [cs.CL]

[47] Hongbo Zhang, Junying Chen, Feng Jiang, Fei Yu, Zhihong Chen, Guiming Chen, Jianquan Li, Xiangbo Wu, Zhang Zhiyi, Qingying Xiao, Xiang Wan, Benyou Wang, and Haizhou Li. 2023. HuatuoGPT, Towards Taming Language Model to Be a Doctor. In *Findings of the Association for Computational Linguistics: EMNLP 2023*, Houda Bouamor, Juan Pino, and Kalika Bali (Eds.). Association for Computational Linguistics, Singapore, 10859–10885. https://doi.org/10.18653/v1/2023.findings-emnlp.725

[48] Renrui Zhang, Jiaming Han, Chris Liu, Peng Gao, Aojun Zhou, Xiangfei Hu, Shilin Yan, Pan Lu, Hongsheng Li, and Yu Qiao. 2023. LLaMA-Adapter: Efficient Fine-tuning of Language Models with Zero-init Attention. arXiv:2303.16199 [cs.CV]

[49] Sheng Zhang, Yanbo Xu, Naoto Usuyama, Hanwen Xu, Jaspreet Bagga, Robert Tinn, Sam Preston, Rajesh Rao, Mu Wei, Naveen Valluri, Cliff Wong, Andrea Tupini, Yu Wang, Matt Mazzola, Swadheen Shukla, Lars Liden, Jianfeng Gao, Matthew P. Lungren, Tristan Naumann, Sheng Wang, and Hoifung Poon. 2024. BiomedCLIP: a multimodal biomedical foundation model pretrained from fifteen million scientific image-text pairs. arXiv:2303.00915 [cs.CV]

[50] Zhenyu Zhang, Benlu Wang, Weijie Liang, Yizhi Li, Xuechen Guo, Guanhong Wang, Shiyan Li, and Gaoang Wang. 2023. Sam-Guided Enhanced Fine-Grained Encoding with Mixed Semantic Learning for Medical Image Captioning. arXiv:2311.01004 [cs.CV]

[51] Long Zhao, Nitesh B. Gundavarapu, Liangzhe Yuan, Hao Zhou, Shen Yan, Jennifer J. Sun, Luke Friedman, Rui Qian, Tobias Weyand, Yue Zhao, Rachel Hornung, Florian Schroff, Ming-Hsuan Yang, David A. Ross, Huisheng Wang, Hartwig Adam, Mikhail Sirotenko, Ting Liu, and Boqing Gong. 2024. VideoPrism: A Foundational Visual Encoder for Video Understanding. arXiv:2402.13217 [cs.CV]

[52] Wayne Xin Zhao, Kun Zhou, Junyi Li, Tianyi Tang, Xiaolei Wang, Yupeng Hou, Yingqian Min, Beichen Zhang, Junjie Zhang, Zican Dong, Yifan Du, Chen Yang, Yushuo Chen, Zhipeng Chen, Jinhao Jiang, Ruiyang Ren, Yifan Li, Xinyu Tang, Zikang Liu, Peiyu Liu, Jian-Yun Nie, and Ji-Rong Wen. 2023. A Survey of Large Language Models. arXiv:2303.18223 [cs.CL]

[53] Zhonghan Zhao, Wenhao Chai, Xuan Wang, Li Boyi, Shengyu Hao, Shidong Cao, Tian Ye, Jenq-Neng Hwang, and Gaoang Wang. 2023. See and think: Embodied agent in virtual environment. *arXiv preprint arXiv:2311.15209* (2023).

[54] Zhonghan Zhao, Kewei Chen, Dongxu Guo, Wenhao Chai, Tian Ye, Yanting Zhang, and Gaoang Wang. 2024. Hierarchical auto-organizing system for open-ended multi-agent navigation. *arXiv preprint arXiv:2403.08282* (2024).

[55] Zhonghan Zhao, Ke Ma, Wenhao Chai, Xuan Wang, Kewei Chen, Dongxu Guo, Yanting Zhang, Hongwei Wang, and Gaoang Wang. 2024. Do We Really Need a Complex Agent System? Distill Embodied Agent into a Single Model. *arXiv preprint arXiv:2404.04619* (2024).